

## University of Rhode Island DigitalCommons@URI

Civil & Environmental Engineering Faculty  
Publications

Civil & Environmental Engineering

2017

# Stronger at Depth: Jamming Grippers as Deep Sea Sampling Tools

Stephen Licht

*University of Rhode Island*, [slicht@uri.edu](mailto:slicht@uri.edu)

Everett Collins

*See next page for additional authors*

Follow this and additional works at: [https://digitalcommons.uri.edu/cve\\_facpubs](https://digitalcommons.uri.edu/cve_facpubs)

**The University of Rhode Island Faculty have made this article openly available.  
Please let us know how Open Access to this research benefits you.**

This is a pre-publication author manuscript of the final, published article.

Terms of Use

This article is made available under the terms and conditions applicable towards Open Access Policy Articles, as set forth in our [Terms of Use](#).

### Citation/Publisher Attribution

Licht, S., Everett, C., Lopes, M. M., & Christopher, B. (2017). Stronger at Depth: Jamming Grippers as Deep Sea Sampling Tools. *Soft Robotics*. 4(4), 305-316. doi: 10.1089/soro.2017.0028  
Available at: <https://doi.org/10.1089/soro.2017.0028>

This Article is brought to you for free and open access by the Civil & Environmental Engineering at DigitalCommons@URI. It has been accepted for inclusion in Civil & Environmental Engineering Faculty Publications by an authorized administrator of DigitalCommons@URI. For more information, please contact [digitalcommons@etal.uri.edu](mailto:digitalcommons@etal.uri.edu).

---

**Authors**

Stephen Licht, Everett Collins, Emmanuel Lopes Mendes, and Christopher Baxter

# Stronger at Depth: Jamming Grippers as Deep Sea Sampling Tools

*Abstract*— In this work we experimentally demonstrate (a) that the holding strength of universal jamming grippers increases as a function of the jamming pressure to greater than three atmospheres, and (b) that jamming grippers can be used for deep sea grasping tasks in ambient pressures exceeding one hundred atmospheres, where such high jamming pressures can be readily achieved. Laboratory experiments in a pressurized, water filled test cell are used to measure the holding force of a 'universal' style jamming gripper as a function of the pressure difference between internal membrane pressure and ambient pressure. Experiments at sea are used to demonstrate that jamming grippers can be installed on, and operated from, remotely operated vehicles (ROVs) at depths in excess of 1200m. In both experiments, the jamming gripper consists of a latex balloon filled with a mixture of fresh water and ~200 micron glass beads, which are cheaply available in large quantities as sand blasting media. The use of a liquid, rather than gas, as the fluid media allows operation of the gripper with a closed loop fluid system; jamming pressure is controlled with an electrically driven water hydraulic cylinder in the lab, and with an oil hydraulic driven large-bore water hydraulic cylinder at sea.

*Keywords*—*soft robotics; compliant grippers; universal jamming gripper; underwater manipulation; remotely operated vehicles.*

## I. INTRODUCTION

Robotic sampling of fragile and irregularly shaped objects is often a critical component of deep sea biological and archaeological investigations. The current state of the art for underwater sampling is the use of one or two manipulators with multiple rigid links and rigid end-effectors driven with high pressure oil hydraulics. Even with highly skilled pilots, collecting samples at any reasonably complex site with an ROV is difficult and time consuming. It is not atypical for a >2000kg robot with a potential grip closure strength of >1000N to be used to sample objects with a weight of only a few grams in water. The fundamental danger in these sampling tasks is that a rigid gripper on a non-back drivable arm could make unintended contact with a priceless, fragile object with a huge amount of momentum driving the gripper and the arm. Soft robotics are attractive in large part because their inherently compliant structures can passively eliminate accidental shock loading on sampled objects.

For the present study, we use a 'universal' particle jamming gripper. Particle jamming is accomplished by creating a pressure differential between the inside of a particle filled flexible membrane and the fluid surrounding the membrane [1]. When the flexible membrane is filled with fluid at the same pressure of the surrounding fluid, the membrane does not obstruct the motion of the particles inside. The particles can move around each other freely, and the membrane is free to take the shape of any object that it is pressed against. To make the membrane harden in its current shape, fluid is removed from the inside of the membrane. The grains inside are jammed together by the membrane, which constricts under the external pressure. The grains can no longer flow around each other and the whole mass becomes rigid.

A universal jamming gripper uses a single elastic membrane filled with particles, where the membrane is suspended below a rigid disc or shallow cup [1]. As shown in Figure 1, the membrane is lowered onto the object to be grasped, fluid is pumped out to jam the particles together, and the object can then be picked up along with the gripper. The performance of universal jamming grippers has been a topic of extensive quantitative characterization in air [2] [3] [4]. It has been commercialized for factory automation Empire Robotics, albeit not yet successfully [5]. Particle jamming has also been proposed and demonstrated in a wide variety of more mechanically complex manipulation applications including, e.g. control of joint stiffness and 2-DOF actuation in pneumatically actuated fingers [6, 7], articulated motion in an octopus like manipulator arm [8], two degree motion in and in a multi-fingered hand [9]. We have chosen to focus on the universal gripper as a test case for jamming grippers at depth for reasons of simplicity and robustness.

Soft robotics is particularly attractive in underwater applications because soft components can have densities close to that of the surrounding fluid. When operated underwater, soft robotics can use liquid, rather than gas, within the internal fluid circuits without making the robot too heavy to support itself. Indeed, an incompressible liquid is required to avoid the use of high pressure gas reservoirs and attendant regulation apparatus which would otherwise be needed to compensate for pressure at depth. The feasibility of using water for both pressure compensation and fluid actuation has been demonstrated at depths greater than 500m with fiber reinforced finger-like actuators [10]. A further benefit of using liquid, as noted in [11] is that it allows the use of a low volume closed-circuit fluid system to control particle jamming, however this was proposed as a means of creating compact terrestrial vehicles. Liquid water as a medium for jamming in a submerged universal gripper was first described in [12] where various objects were recovered from the bottom of a 4m deep fresh water tank.

Intriguingly, [1] hypothesized that the strength of the grasp of a universal jamming gripper should be linear function of the vacuum pressure with respect to the ambient air, particularly for the case where an interlocking grasp was achieved on a sample. The mechanism postulated was an increase in the shear strength of the jammed mass as the jamming pressure increases. Given that the jamming pressure is limited by the absolute ambient pressure, and that ambient pressure increases with water depth, a particle jamming based gripper should increase in strength as it is carried deeper in the water column, making it an attractive choice as a deepwater tool.

The experiments described below were performed to test the hypotheses that (a) the maximum lifting force that can be achieved by a universal jamming gripper is dependent on the jamming pressure, i.e. the pressure drop across the confining membrane between ambient and internal; that (b) this increase in gripper performance occurs when the ambient and interstitial internal fluid consists of liquid water; and that (c) the force continues to increase for jamming pressures greater than one atmosphere.

## II. METHODS

Our goal in developing underwater soft gripper technologies is to support deep water archaeological and biological sampling, particularly deep water intervention tasks using remotely operated vehicles (ROVs) tethered to a surface ship. Our target platform is the scientific work class ROV *Hercules*, pictured in Figure 2, which can be

operated to depths of up to 4000m from the dedicated 64-m support ship E/V *Nautilus*<sup>1</sup>. The ROV pilots aboard the surface ship communicate with and command the actuators and sensors onboard the ROV via the tether. The ROV *Hercules* uses electric power transmitted over the tether to drive onboard systems, including a 15-kW rated hydraulic pressure unit (HPU) capable of supply pressures up to 3000psi. A Kraft Predator™ 7-DOF hydraulic arm with a rigid pincer end-effector is used for all physical sampling tasks. Samples are either grasped directly with the end-effector, or acquired using tools that can be picked up by the end effector from the ROV 'front porch'. The Kraft arm uses joint fluid pressure to transmit force information to the pilot's control joystick, however pilots are justifiably reluctant to rely on the rigid end-effector to grasp potentially priceless, non-renewable cultural artifacts. In this effort, we focus on a 'universal' style jamming gripper which can be picked up and applied by the rigid end-effector, as shown in Figure 3.

The gripper design includes a linear bearing, which limits the maximum vertical force applied to any sample to the in-water weight of the gripper itself. A closed-circuit hydraulic system converts high-pressure, low volume oil hydraulics to low-pressure, high volume water hydraulics through an in-line cylinder pair. A schematic showing the design of the gripper membrane, manifold, cap, and handle is shown in Figure 4. The fluid manifold is machined from a 6061aluminum rod and connects a single inlet-outlet port from the side to an internal cavity bored out from the bottom of the manifold. The bottom hole is covered with a filter (400x400 mesh stainless steel woven wire cloth) that allows water flow but blocks the particles from entering the manifold. The manifold is inserted through the cap (3-D printed in ABS using a Stratsys Dimension printer) and then in to the neck of a latex balloon (Qualatex 18" Diamond Clear Round) that is partially filled with 94g of solid glass beads (Potters Ballotini® 212-300µ Impact Beads). The average density of the bead material is 2.5g/cc, the average density of the packed beads is 1.66g/cc, and the uninflated volume of the membrane is approximately 225cc. The beads are thus 25% of maximum amount that can be contained without inflating the membrane. A blind threaded hole in the top of the cylinder is used to attach to the gripper handle shaft of nominal 0.5in diameter ceramic-coated aluminum.

The fluid drive system consists of a 127mm bore stainless steel water filled cylinder (TRD Mfg., RS Series) and a 25mm bore oil filled cylinder (HydroLek 11060). The piston rods of the two cylinders are concentric and directly connected end to end, as indicated in cross-section in Figure 4. A three-position four-way proportional valve, which is integrated with an existing 1500psi oil-hydraulic system on-board the ROV, is used to control the high pressure cylinder. The maximum jamming pressure across the jamming membrane is 58psi (3.95atm), resulting from the hydraulic system pressure of 1500psi and the 26:1 area ratio of the two cylinders. The pilot controls the valve from the surface through manual setting of the solenoid valve PWM duty cycle; fine control of jamming pressure was not possible during the experiments described here due to the nearly 10 second latency in valve control and pressure response. Jamming pressure was observed using an analog gauge pressure sensor (Thuemling SPAN series) referenced to ambient pressure with a range of ±60psi (±414kPa). The installed locations on the *ROV Hercules* of the gripper apparatus, the fluid drive system, the analog pressure gauge, all of which are connected using flexible thick walled polyurethane tubing (1.8in ID, 3/8in OD), are indicated in Figure 5.

---

<sup>1</sup> <http://www.nautiluslive.org/tech>

A linear bearing was used to enable the robot manipulator to apply full strength upwards while at the same time passively limiting the downwards force applied to the in-water weight of the gripper apparatus. The gripper handle shaft slides in the linear bearing, and is constrained in the downward direction by a shaft collar clamped around the top of the shaft. In field operation, the robot manipulator grasps the apparatus via the outer bearing cylinder which has a plain thrust bearing (Rulon J self-lubricating PTFE) press fit into each end. Handling with the pincer mechanism is made easier by the addition of two 2.5in (64mm) diameter rigid polyurethane ball handles to the bearing cylinder, as shown in the image Figure 3, which gives the pilots view of operations when the ROV is at depth.

As illustrated in Figure 1, the weight of the gripper and its load are supported by the shaft collar when the gripper is not in contact with the substrate. The arm is then lowered until the weight of the gripper is fully supported by the sample and/or substrate. The pilot can see that this has occurred by observing when the bearing cylinder begins sliding down the shaft, thus losing contact with the shaft collar. Once the gripper is in contact, fluid is removed from the membrane via the fluid inlet port, developing a pressure difference across the membrane and jamming the particles.

For the deployed gripper, and for all experiments in this effort, the membrane was only partially filled with particles. As described in [12] the partially filled membrane is able to drape around the objects that it is applied to, and the weight of the freely flowing particles then forces the membrane to extend slightly underneath overhangs. This shape promotes the gripping modality referred to in [1] as 'interlock', as opposed to the 'friction' and 'suction' modes. The interlock mode is the mode that is most clearly dependent on the shear strength of the rigid gripper shape, as the grip fails only with large scale shape changes. For the purposes of this effort, the primary effect of this design choice is that the partially filled membrane achieves an effective interlocking grip without the need to shape the membrane around the object, whether manually as in [1], or with some additional actuation step which would add potentially unacceptable complexity to fielded operation.

One consequence of the use of a partially filled membrane is that there is a significant difference in the volume of the membrane before and after the jamming step, as illustrated in Figure 1 (b)-(c). In order for the gripper to achieve a high quality grasp on the object, it is critical that the apparatus be free to fall under its own weight and thus continue to press down on the membrane as the fluid is removed. In previous work [12] this was accomplished by allowing the cap to slide on the manifold, but pinching of the membrane between the cap and the manifold during the relative motion was found to be a primary failure mode. For this effort, the membrane and cap move together as the bearing shaft slides within the bearing cylinder. This proved to be a more reliable solution and made it possible to change the total range of motion simply by increasing the shaft length.

### III. EXPERIMENTAL APPARATUS: LABORATORY

As operational time at depth on a work class scientific ROV is extremely costly, the gripper design was extensively tested using a triaxial load frame (GeoComp LoadTrac-II) with an integrated pressure chamber and flow control system (GeoComp FlowTrac-II). The experimental apparatus is pictured in Figure 6. The pressure chamber is an acrylic cylinder with gasket-sealed removable top and bottom caps. The pressure chamber is mounted rigidly to the movable platen of the load frame. The platen can follow pre-programmed velocity or force profiles, where force is

measured using a single-axis S-beam load cell mounted to the load frame above the pressure chamber, and velocity is measured using a spring loaded linear probe in contact with the platen.

The top cap of the pressure chamber contains a shaft penetration consisting of a linear bearing with a dynamic o-ring seal. The gripper apparatus is contained inside the pressure chamber, supported from above by the gripper handle, which passes through the shaft penetration. Two fluid inputs to the chamber, accessed through fittings in the bottom cap, are connected externally to two independent FlowTrac-II systems, which consist of electrically driven water hydraulic cylinders instrumented for pressure and volume control. One flow control system is plumbed directly to the interior of the pressure chamber, and controls ambient chamber pressure. The other flow control system is plumbed to a pass through, which is connected inside the chamber to a length of flexible tubing, which is in turn connected to the manifold. The flexible tubing is arranged in a spiral configuration to minimize vertical forcing on the gripper. The fluid circuits are isolated from one another and closed. All fluid used in these experiments is fresh water at room temperature.

The manifold, cap, membrane, and beads tested are identical to those used at sea, however a longer handle shaft is needed to provide sufficient length to protrude from the pressure chamber regardless of the gripper vertical position relative to the chamber. Eyebolts are threaded in to the bottom of the S-beam load cell (Artech 20210 series, max. load 11N) which is attached to the load frame above the chamber, and in to the top of the gripper handle shaft. A weight tray is mounted to the lower shaft, allowing weight to be added to compensate for the vertical pressure force resulting from chamber pressures which are higher than the ambient pressure in the laboratory. The pressure force is proportional to this pressure differential and the internal cross-sectional area of the linear bearing.

The sample object in all tests is a 110mm long, 10mm diameter stainless steel tube. The sample was mounted parallel to the surface of the aluminum base plate, with the lower surface held 6mm above the substrate with a 4-40 rod, which was threaded into a blind tapped hole in the center of the length. During all experiments the rigid cone of the gripper apparatus makes contact with the ends of the sample rod. As a result, the entire weight of the gripper apparatus rests on the sample, with the exception of some portion of the bead and membrane weight which is supported by the substrate. The downward load on the sample is thus approximately equal to the in-water weight of the gripper. This sample geometry was chosen to simplify estimates of the downwards force applied, eliminating the need for a submersible force sensor to distinguish between loads applied to the sample and the substrate.

For each experiment, as shown in Figure 7, the gripper mechanism is allowed to come to rest on the sample before jamming, and to settle on the sample during jamming, under the weight of the gripper mechanism, shaft, and weight tray. Once the gripper is fully jammed, the shaft is connected to the load cell by a tension member, and the platen is lowered until the jammed gripper loses contact with the sample. In this manner, we are able to measure the total upwards force applied by the gripper to the sample, while ensuring that the downward force applied does not exceed the total in water weight of the gripper and the handle, thus simulating operation at sea. Gripper holding force is calculated as the difference between the maximum load recorded by the load cell, and the load recorded immediately after all contact with the sample is lost, with the platen still in downward motion.

The two flow control systems are used to independently control pressure and flow inside the membrane and surrounding the membrane. Throughout each experiment, the chamber pressure was regulated by injecting or removing fluid using PID feedback control, with external piston volume as the control input. The volume of fluid external to the membrane is directly tied to the total displacement of the gripper and the gripper support structure; thus when fluid is added or removed from the membrane to control either membrane volume or membrane pressure, fluid must be removed or added to the chamber to maintain pressure. Lowering or raising the gripper structure changes the displacement of the gripper, as the shaft penetrates to different distances, again requiring fluid to be removed or added.

The membrane fluid flow is used to regulate either volume or pressure depending on the current stage of the grasping process. Prior to grasping, fluid is removed from the membrane in pressure regulation mode to achieve a small (10kPa) difference between internal and external pressure, indicating the start of jamming. A controlled volume of fluid is then injected in to the membrane to inflate it partially prior to application to the sample. This initial fluid volume is one of the parameters varied in the experiments described below. All tests are performed with the starting internal membrane pressure equal to the surrounding ambient pressure, as the balloon is never inflated to the point of elastic stretching. Once the gripper is applied to the sample, the gripper is 'jammed' by removing fluid from the membrane, regulating pressure to achieve the desired jamming pressure.

#### IV. LABORATORY EXPERIMENT: RESULTS

The gripper lifting force,  $F_L$ , was recorded while varying four experimental parameters: system weight in water,  $F_W$ , ambient pressure,  $P_A$ , jamming pressure,  $P_J$ , and initial membrane fluid volume  $V_I$ . A series of 23 experiments was performed.

##### *Jamming pressure.*

We recorded  $F_L$  as a function of  $P_J=(30, 60, 85, 170, 255, 340)$  kPa with  $P_A = 4$  atm,  $F_W = 5$ N, and  $V_I = 120$ mL. As seen in Figure 8,  $F_L$  increases more than three-fold, from 3.8N to 15.3N when  $P_J$  is increased from 30 to 85kPa.  $F_L$  doubles again to 29.9N when  $P_J$  is increased to 340kPa. The relationship is linear within the upper range; recorded mean values with error bars representing variance are plotted against a linear fit to the experiments within this range, where  $F_L = 0.057 \times 10^{-3} P_J + 10$ . There is a significant difference in sensitivity above and below  $P_J = 85$ kPa, and the linear fit to the lower range is  $F_L = 0.21 \times 10^{-3} P_J - 2.6$ .

##### *Effects of ambient pressure.*

To determine sensitivity of  $F_L$  to ambient pressure, three experiments were performed at reduced ambient pressures for a subset of the jamming pressures above,;  $P_J=85$ kPa at 1atm, and  $P_J=(85, 170)$  kPa at 2atm.  $P_J$  cannot exceed the ambient pressure in any experiment.  $V_I=120$ mL was maintained in order to ensure that the initial volume threshold for repeatable gripper performance was met, based on the results of tests across varying  $V_I$  described below. There was no significant change in the gripper performance when  $P_A$  is varied between 1, 2, or 4atm, as seen in Figure 8. Results from the three field trials described below, with  $P_A \approx 120$ atm and  $P_J=404$ kPa, also shown for comparison in



Figure 8, and are consistent with the linear fit developed between  $F_L$  and  $P_J$  at  $P_A=4\text{atm}$ , suggesting that the  $F_L$  is independent of  $P_A$  across two orders of magnitude in  $P_A$ .

#### *Initial membrane volume.*

We recorded  $F_L$  as a function of  $V_I=(40, 80, 100, 120, 140, 160)$  mL, while holding  $P_A=4$  atm and drawing  $P_J=340\text{kPa}$ .  $F_L$  increased monotonically with  $V_I$ , ranging from an average of 18N at  $V_I=40\text{mL}$  to 34N at  $V_I=160\text{mL}$ , as seen in Figure 9. Using  $n=5$  trials for each operating condition, we found that measured  $F_L$  was repeatable for  $V_I=100$  mL and higher. In contrast, for  $V_I=100\text{mL}$  and lower, the results show much higher variability, with an apparently bimodal distribution of measured  $F_L$ . For the lowest initial volume, individual trials ranged from a minimum of 9N to a maximum of 23N. Images of the membrane at four different stages are shown in Figure 11 for one trial each with  $V_I=40$  and  $V_I=120\text{ml}$ , resulting in  $F_L=9\text{N}$  and  $F_L=30\text{N}$ , respectively. The membrane shape just before contact with the sample is closer to symmetric with  $V_I=120\text{mL}$ , without the sharp folds evident when  $V_I=40\text{mL}$ . For  $V_I=120\text{mL}$  and above, the membrane prevents the cap from making contact with sample before jamming, and is slightly pressurized from holding gripper weight; the membrane is also more compact and symmetrically positioned around the sample once jammed.

#### *System weight.*

We tested the sensitivity of gripper performance to system weight,  $F_W$ , first by varying  $F_W$  and  $P_J$  while holding  $V_I$  constant (see Figure 8) and then by varying  $F_W$  and  $V_I$  while holding  $P_J$  constant (see Figure 9.)  $F_W$  was increased to 10 N with  $P_J=(30, 85, 340)$  kPa, holding constant  $P_A=4\text{atm}$ , and  $V_I=120$  mL. In each case, mean gripper lift strength varied by less than 1N when the system weight was increased. We recorded  $F_L$  for  $F_W=(1, 10)$  N with  $V_I=(40, 120)$  mL, holding constant  $P_A=4\text{atm}$ , and  $P_J=340\text{kPa}$ . Gripper lift strength varied by less than 2N between the three system weights for the case where  $V_I=120\text{mL}$ . For  $V_I=40$  mL and lower system weight  $F_W=1\text{N}$ ,  $F_L$  remained bimodal, with similar maximum and minimum values compared to the case where  $F_W=5\text{N}$ . For the higher system weight, however, the results were repeatable for  $n=5$ , and the mean value of all trials matched the higher of the two modes for the case where  $F_W=5\text{N}$ .

## V. FIELD TESTS

In July 2016, we were able to deploy the gripper prototype on the ROV *Hercules* during the E/V *Nautilus* field campaign at the Southern California Margin. The gripper was tested at depth, where it successfully grasped a number of man-made and naturally occurring objects at the sea floor. We modified the gripper shown in Figure 3 to allow for in-situ measurement of the lifting force, using the target object from experimental program described above.

The stainless steel rod sample target was mounted on a flat PVC disc on the front porch of the ROV *Hercules*, again parallel to the surface at a height of 6mm. Two stainless steel linear compression springs were installed on longer gripper handle shaft, between the shaft collar and the linear bearing as pictured in Figure 12(a). Solder was wrapped around the cap of the gripper to increase in-water weight of the modified gripper apparatus to 5N.

The ROV manipulator was used to lower the gripper on to the sample from above, and then fluid was removed from the membrane to jam the gripper. The ROV manipulator was then used to raise the bearing cylinder. Each of the

spring in series was compressed by the combined force of the gripper weight and the vertical force applied by the sample on the gripper. Initial fluid volume could not be either precisely controlled or accurately measured; the on/off control channel for fluid injection was subject to an approximately 10 second lag, and feedback was entirely based on observing the outside of the membrane through the ROV main camera. Before each experiment, fluid was injected in five second bursts until the membrane appeared to be smooth and slightly inflated, ensuring  $V_I > 120\text{mL}$ .  $P_J = 404\text{kPa}$  (4 atm) was repeatably reached in all trials by actuating the drive cylinder long enough to ensure that full pressure was reached within in the high pressure piston, resulting in maximum jamming pressure in the water hydraulic system.

Gripper strength,  $F_L$ , was measured by using the maximum length change in the lower spring when compared to the length of the spring under the gripper weight alone. The linear spring constant,  $k$ , for the lower spring was found to be  $k = 0.60\text{N/mm}$  during testing prior to deployment. The deformation of the upper spring cannot be used as it is clearly compressed beyond the linear compression range. The vertical length of the upper plain bearing was taken as a reference length of 25.4mm (1.0in), to account for changes in camera view angle. Three trials were performed on this target with the ROV at a depth of 1200m, i.e. with an ambient pressure  $> 120$  atm.

$F_L = 32\text{N}$ ,  $38\text{N}$ , and  $35\text{N}$  for trials I, II, and III, respectively, based on isolated images in video frame captures as shown in Figure 12. While all operations were performed by the same ROV pilot in an attempt to maintain consistent trajectories across trials, the manipulator was manually controlled, resulting in motions that were not exactly vertical. An image showing the typical shape of the gripper immediately after grip failure is shown in Figure 14. The results from all three individual trials are plotted along with the results from laboratory experiments in Figure 8 for comparison. While these are necessarily relatively crude estimates given the significant sources of measurement error and unavoidable variability in gripper motion, the measured gripper performance is consistent with the linear relationship developed from experiments performed at much lower ambient pressures.

## VI. DISCUSSION

We make a number of observations related to the combined laboratory and field experiments, and expand on them below:

- (1) Better gripper performance can be achieved at higher ambient pressures.
- (2) For a given jamming pressure, gripper strength is independent of ambient pressure.
- (3) Gripper strength increases with increased initial fluid volume, and grasping is more reliable above a threshold initial fluid volume.
- (4) Gripper pull strength is insensitive to system weight.
- (5) Interaction of target shape with operational parameters is a necessary area of future investigation.

### *1) Better gripper performance can be achieved at higher ambient pressures.*

The lifting force of the gripper increases with the jamming pressure, regardless of the ambient pressure. The jamming pressure must be lower than the ambient pressure. Therefore higher ambient pressures make it possible to achieve higher grip strengths, subject to the limits of the mechanisms used to create the jamming pressure differential. When operating at sea level jamming pressure is limited to less than 101kPa. When submerged in water, ambient pressure increases by approximately 1atm for every 10m increase in depth. In laboratory tests, gripper lifting force

doubled as jamming pressure increased from 85kPa, which can be achieved at sea level, to 340kPa, which can be only be achieved at water depths greater than 24m.

If we assume that the failure mode is shear failure at the base of the interlock tabs that extend underneath the sample, we are able to make a first order prediction of the holding strength based on the estimated material properties of the jammed particles. The force required to cause shear failure should be proportional to the ultimate shear strength of the material,  $\tau$ , and the area,  $A_{shear}$ , of the shear plane according to  $F_L = \tau A_{shear}$ .

We assume  $\tau$  for the jammed particulate mass is proportional to the effective stress according to the Mohr-Coulomb failure criterion,  $\tau = \sigma' \tan \phi'$ , where  $\phi'$  is the effective stress friction angle [13]. For  $\sigma' = P_J$ , we expect  $F_L = P_J \tan \phi' A_{shear}$ . We assume that the geometry of the gripper is constant after jamming occurs, and can thus treat  $A_{shear}$  as independent of jamming pressure. The length of the tabs along the sample is on the order of two diameters of the sample rod (20mm), as shown by the view from below in Figure 14, and the thickness of the tabs protruding beneath the sample cannot exceed the height of the sample rod (6mm), implying that the two tabs would have a maximum combined shear area of approximately 480mm<sup>2</sup>.  $\phi'$  for fine spherical glass beads is taken to be 32 degrees [13]. Using the slope of the linear fit to the recorded lifting force below 85kPa jamming pressure, we would expect that the area of the shear plane is on the order  $A_{shear} = 320 \text{ mm}^2$ .

This first order prediction does not, however, adequately account for the abrupt change in sensitivity to  $P_J$  above 85kPa. A possible explanation for this discrepancy highlights one difference between jamming in air and in water, which is that liquid water is effectively incompressible. Because the membrane is sealed after  $P_J$  is applied and the water is incompressible, any deformation of the jammed particles during lifting occurs under constant volume conditions. Depending on the initial packing of the particles, there will be a tendency for volume change during lifting (i.e. shear) that will result in a corresponding change in pore pressure [13]. The pore pressure that develops modifies the effective stress on the jammed particles in the membrane, and at the failure point,  $\sigma' \neq P_J$ , if  $P_J$  is the pressure drop across the membrane when the volume is sealed.

Change in pore pressure during gripper loading was available from a pressure tap during two trials at initial jamming pressures,  $P_J=85\text{kPa}$  and  $P_J=340\text{kPa}$ . The change in pore pressure as a function of gripper displacement is shown in Figure 15 for these two cases, with the pressure occurring at maximum recorded lifting force highlighted for each. At  $P_J=85\text{kPa}$ , the membrane internal pressure has increased by 5kPa when failure occurs, reducing  $\sigma'$  to 80kPa, a 6% drop from the initial value. At  $P_J=340\text{kPa}$ , the pressure has increased by 65kPa when failure occurs, reducing  $\sigma'$  to 275kPa, a 19% drop from the initial value. These results indicate that the assumption that  $\sigma_{eff} = P_J$  overstates the effective pressure for jamming pressures above 85kPa.

The results are also consistent with the fact that, for a given packing of particles, at low effective stresses the particles have a tendency to dilate during shear, which will inhibit pore pressure development and can even lead to negative pore pressures. At higher effective stresses, however, the particles have a tendency to contract during shear, with corresponding positive pore pressures. This transition from dilatative to contractive behavior of the particles during constant volume shear may explain the change in slope in Figure 8.

2) *For a given jamming pressure, gripper strength is independent of ambient pressure.*

The relationship between the lifting force of the gripper and the ambient pressure is indirect, and is entirely dependent on the fact that ambient pressure serves as a hard limit to jamming pressure. Varying the ambient pressure within the test cell between 1atm and 4atm had no apparent effect on the gripper pull strength for a given jamming pressure. At a water depth of 1200m, the ambient pressure exceeds 100atm. Trials performed at that depth, although limited in scope, closely follow the linear relationship between jamming pressure and gripper strength found with ambient pressures two orders of magnitude lower, supporting this conclusion.

3) *Gripper strength increases with increased initial fluid volume, and grasping is more reliable above a threshold initial fluid volume.*

The importance of initial fluid volume is shown by the increase in lifting force from 18N to 34N across the range of volumes tested. Notably, however, at and below 100mL there is a significant chance that the gripper will fail to achieve an effective grasp on the sample, resulting in lifting force as low as 9N. Recalling that the uninflated volume of the membrane is 225mL, and that the beads and interstitial fluid surrounding them occupy 25% of that volume the membrane is 69% full when  $V_I = 100\text{mL}$ . Based on images of the membrane shape before and after contact, we believe that this represents a threshold above which the elastic membrane forms around the sample in an organized, symmetric fashion, possibly due to the slight inflation of the membrane required to support the weight of the apparatus. Where the initial volume is too low, deeper folds and asymmetries in the membrane prior to and after contact may make the success of the grasp highly sensitive to rotation of the gripper apparatus about the vertical shaft.

4) *Gripper pull strength is insensitive to system weight.*

Experiments performed above the initial volume threshold suggest that the gripper performance does not depend on the system in water weight, across an order of magnitude (from 1 to 10N). For the higher initial fluid volumes (120mL and above) the weight of the system is entirely supported by the internal pressure of the inflated membrane prior to jamming, as shown in Figure 11-b. However, the full weight of the system is applied to the sample as the fluid is removed from the membrane and the cap comes to rest on the ends of the sample. This result suggests that system in water weight can and should be minimized, potentially reducing downwards force without reducing gripper performance.

5) *Interaction of target shape with operational parameters is a necessary area of future investigation.*

It is important to recognize that the discussion above, particularly as related to (3) and (4), comes with the caveat that a single regularly shaped object was used as the grasping target. Targets with dimensions smaller than the cap diameter are of particular interest. The membrane of a partially filled gripper may be able to form around a small target without ever resting the entire weight of the gripper on the target. In that case, higher system weights and higher initial fluid volumes may generate higher internal membrane pressures; even if the rigid portion of the gripper never contacts the sample, a pressurized membrane will still transmit the weight of the gripper to the target.

Grippers for objects resting on soft substrates, such as fine bottom sediment and water logged ship timbers, must minimize downward forces or risk burying their targets. There is a design imperative to minimize gripper weight and

initial fluid volume if it can be done without unduly reducing gripper strength. The influence of initial volume and gripper weight on performance for different target geometries is thus a necessary area of future work.

## VII. CONCLUSION

In this effort we demonstrate that the universal jamming gripper is a viable deep water sampling technology. The performance of jamming grippers in a lifting task is shown to improve with operational depth through experiments in a pressure chamber and as deployed on the *ROV Hercules* at a water depth of 1200m. Jamming gripper performance improves at depth because the maximum holding force that can be sustained is dependent on the jamming pressure, and higher ambient pressures allow higher jamming pressures to be reached. Extreme changes in ambient pressure, from 1 atm at the surface to over 100 atm below 1000m depth, dictate the use of an incompressible liquid as fluid media, but this also provides the opportunity to use a piston driven closed-circuit system to actuate jamming. Piston driven systems are readily installed, actuated, and pressure compensated on any ROV with a high pressure oil hydraulic system. The design of a universal gripper that can be used by an ROV manipulator is shown to be mechanically straightforward, with no actuated mechanical components.

ROV size typically increases with depth rating; as the robot travels deeper, the individual components increase in size and mass to withstand increasing pressure, and the tether itself becomes heavier. ROV size is also driven upwards by the need to do as much as possible on each dive to justify ship operational costs. Ship costs can easily exceed US\$50,000/day, thus a dive to and from a depth of 1000m at 0.5m/s, plus an hour of launch and recovery time, costs in excess of US\$5,000 before the first task is even attempted. Soft manipulators and grippers have the potential to (a) reduce exploration cost by eliminating tool changes while collecting samples with complex and variable geometry, and (b) allow safe sampling of fragile biological and cultural artifacts in the deep-sea.

## ACKNOWLEDGMENT

This study was funded in part by the U.S. Naval Sea Systems Command (NAVSEA) through the Naval Engineering Education Consortium Grant # N00174-15-C-0024 to S.L. The authors would like to express their appreciation to the Ocean Exploration Trust for providing access to the E/V *Nautilus* and the ROV *Hercules*, and to Will Sellers, Wendy Snyder, Matthew Jewell, and Jessica Sandoval, for their skilled piloting of the ROV and the manipulator arm.

## VIII. REFERENCES

- [1] A. Brown, N. Rodenberg, J. Amend, A. Mozeika, E. Steltz, M. Zakin, H. Lipson and H. Jaeger, "Universal robotic gripper based on the jamming of granular material," *PNAS*, vol. 107, no. 44, pp. 18809-18814, 2010.
- [2] J. Kapadia and M. Yim, "Design and performance of nubbed fluidizing jamming grippers," in *IEEE International Conference on Robotics and Automation*, Bielefeld, 2012.
- [3] Y. Jiang, J. Amend, H. Lipson and A. Saxena, "Learning hardware agnostic grasps for a universal jamming gripper," in *IEEE International Conference on Robotics and Automation (ICRA)*, 2012.
- [4] J. Amend, E. Brown, N. Rodenberg, H. Jaeger and H. Lipson, "A Positive Pressure Universal Gripper Based on the Jamming of Granular Material," *IEEE Transactions on Robotics*, vol. 28, no. 2, 2012.
- [5] J. Amend, N. Cheng, S. Fakhouri and B. Culley, "Soft Robotics Commercialization: Jamming Grippers from

Research to Product," *Soft Robotics*, p. 144:158, September 2016.

- [6] Y. Wei, Y. Chen, T. Ren, Q. Chen, C. Yan, Y. Yang and Y. Li, "A Novel, Variable Stiffness Robotic Gripper Based on Integrated Soft Actuating and Particle Jamming," *Soft Robotics*, vol. 3, no. 3, pp. 134-143, July 2016.
- [7] A. Jiang, G. Xynogalas, P. Dasgupta, K. Althoefer and T. Nanayakkara, "Design of a variable stiffness flexible manipulator with composite granular jamming and membrane coupling," in *2012 IEEE/RSJ International Conference on Intelligent Robots and Systems*, Vilamoura, 2012.
- [8] N. Cheng, M. Lobovsky, S. Keating, A. Setapan, K. Gero, A. Hosoi and K. Iagnemma, "Design and Analysis of a Robust, Low-cost, Highly Articulated manipulator enabled by jamming of granular media," in *IEEE International Conference on Robotics and Automation (ICRA)*, Hong Kong, 2012.
- [9] J. Amend and H. Lipson, "The JamHand: Dexterous Manipulation with Minimal Actuation," *Soft Robotics*, vol. Online ahead of print., 2017.
- [10] K. C. Galloway, K. P. Becker, B. Phillips, J. Kirby, S. Licht, D. Tchernov, R. J. Wood and D. Gruber, "'Soft Robotic Grippers for Biological Sampling on Deep Reefs,'" *Soft Robotics*., January 2016.
- [11] A. Jiang, T. Aste, P. Dasgupta, K. Althoefer and T. Nanayakkara, "Granular Jamming With Hydraulic Control," in *37th Mechanisms and Robotics Conference*, Portland, 2013.
- [12] M. Lopes-Mendes, E. Collins and S. Licht, "Universal Jamming Grippers for Deep-Sea Manipulation," in *OCEANS16/IEEE MTS*, Monterrey, California, September 2016.

[13] 150

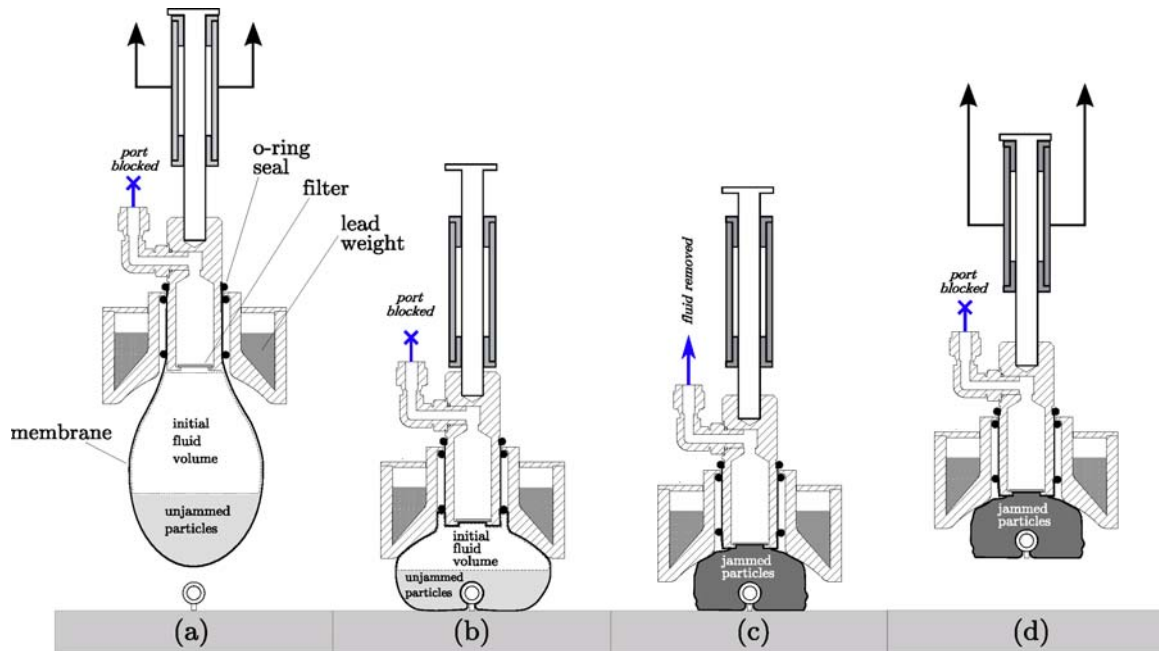


Figure 1: Grasp and recovery of an object using a partially filled jamming gripper with weight-limited downwards force. The gripper is positioned using a robotic manipulator which holds a cylindrical bearing installed on the handle shaft. (a) Prior to contact with the object and the substrate, the membrane contains an initial fluid volume at the ambient pressure, in addition to the fluid surrounding the unjammed particles. The weight of the gripper apparatus is supported by the top of the bearing, which is in contact with a collar at the top of the handle shaft. (b) Upon contact, the jamming gripper membrane conforms to the object and the substrate under the weight of the apparatus. The bearing slides down the handle shaft, keeping the shaft aligned vertically without applying vertical force. (c) Fluid is removed from the membrane until the desired jamming pressure is reached, jamming the particles into a rigid shape. The gripper apparatus settles down on to the particles under its own weight as the fluid is removed, ensuring that the jammed shape remains conformed to the object rather than pulling up and away. (d) The object is picked up along with the gripper apparatus.

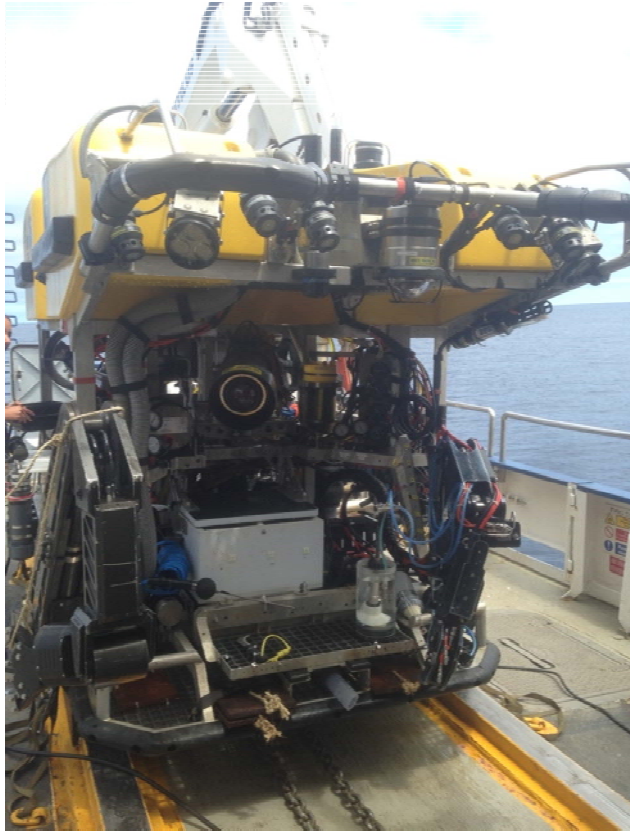


Figure 2: The remotely operated vehicle (ROV) *Hercules* is a science work-class ROV deployed from the dedicated 64m support ship *E/V Nautilus*, operated by the Ocean Exploration Trust. The gripper, fluid drive, and pressure gauge were installed in the port-forward lower corner of the ROV (see detail in Figure 5.) The manipulator arm used to operate the gripper is stowed at the starboard-forward corner (to the left in the view shown.)



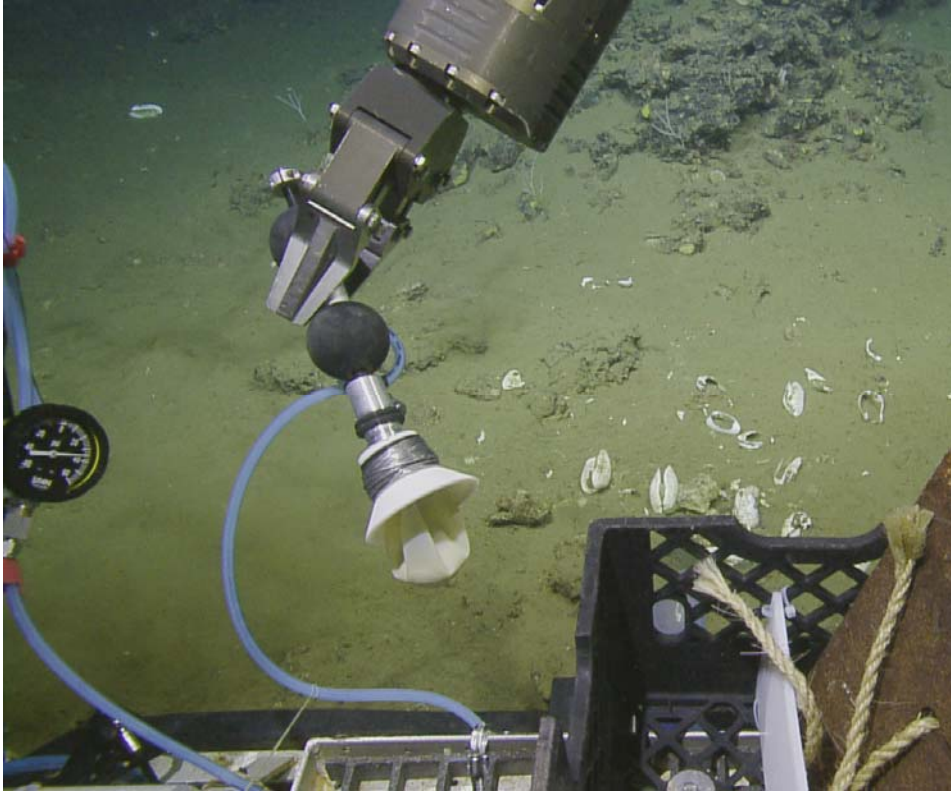


Figure 3: Image of the gripper held by the manipulator, captured from the main camera view used by the ROV pilot. Two 2.5in diameter rigid polyurethane balls are mounted on the cylinder bearing handle to give the manipulator pincer a secure grasp. The flexible blue polyurethane tubing connects the membrane to the pressure gauge to the left of the image, and to the fluid drive system out of view to the left.

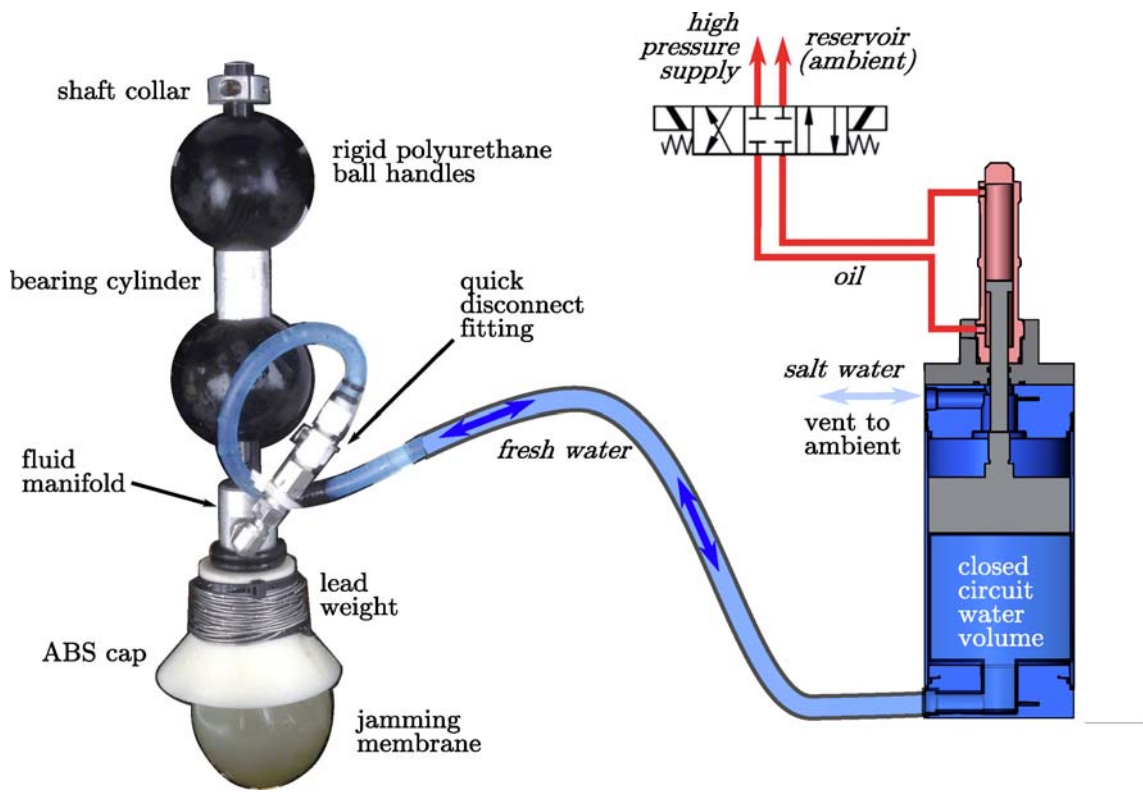


Figure 4: Annotated schematic of gripper apparatus and fluid drive system.

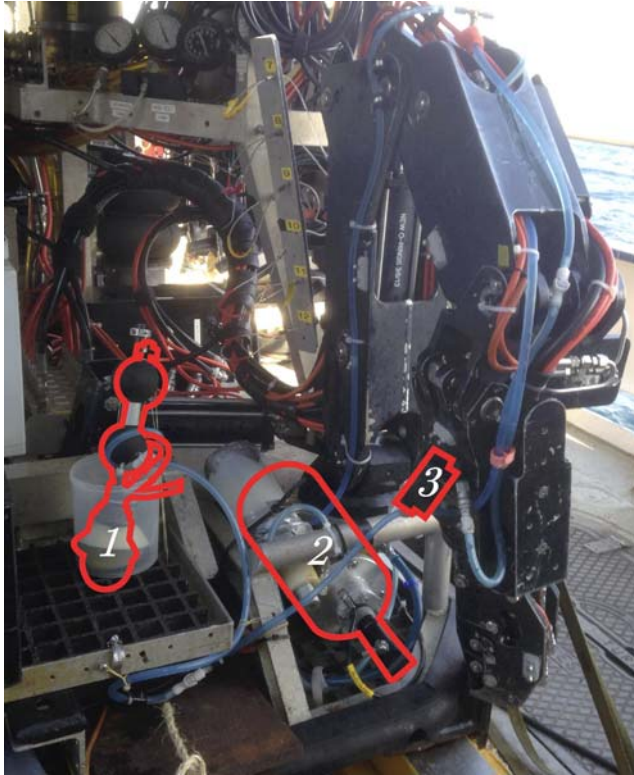


Figure 5: Detail of *ROV Hercules* showing installed location of three components: 1 -gripper, 2- fluid drive system, 3- membrane internal pressure gauge. The gripper itself is resting in an open container on the 'front porch' of the ROV. The fluid drive system is partially occluded in this view. The pressure gauge showing pressure across the gripper membrane is mounted to the secondary manipulator arm, allowing it to be repositioned within the camera field of view during operation of the gripper.

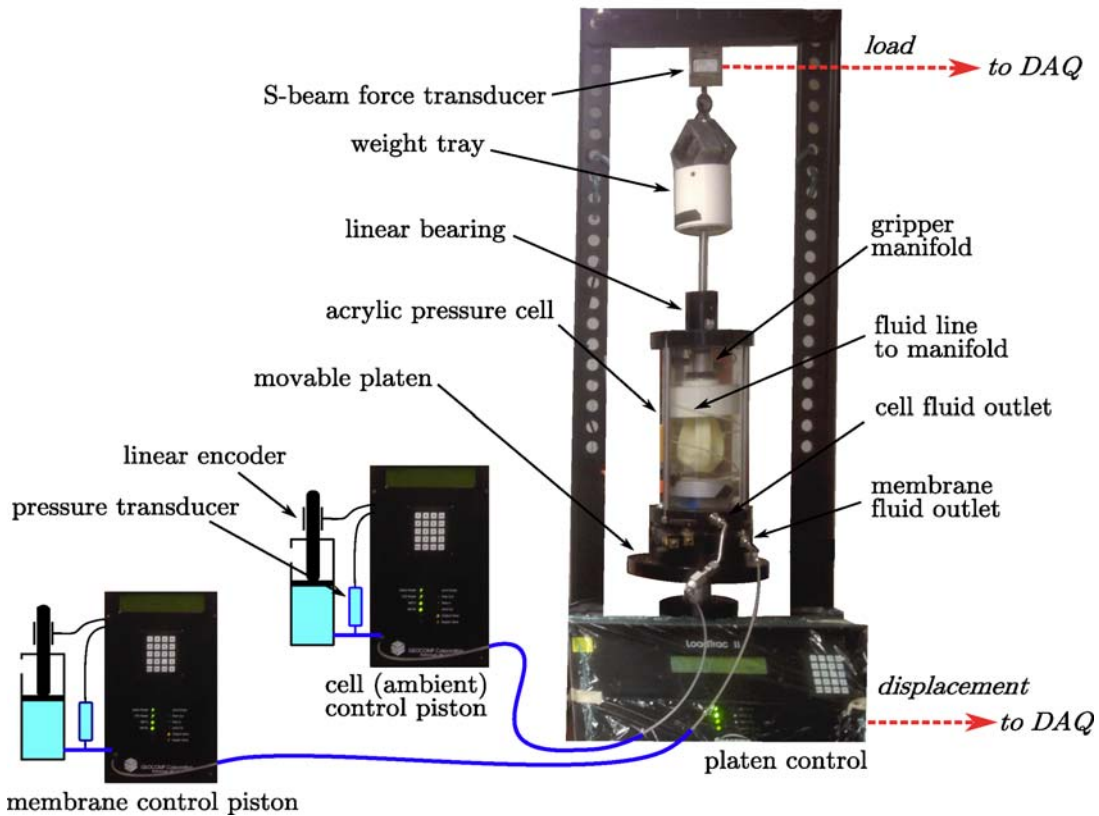


Figure 6: Annotated schematic of bench top gripper experiments in a pressurized water chamber. The object to be grasped is rigidly mounted to the lower section of the pressure chamber, which is in turn rigidly mounted to the movable platen. The gripper is supported by the shaft which runs through the linear bearing in the upper cap of the pressure chamber. Weights in the weight tray compensate for the upwards force caused by difference between the elevated pressure inside the chamber and ambient air pressure in the lab. Two FlowTrak II controllers are used to set either pressure or volume in the chamber and in the membrane. Control of each independent closed (fixed fluid mass) system is accomplished by driving the cylinder connected to that fluid volume. The motion of the gripper and the platen are described in Figure 7.

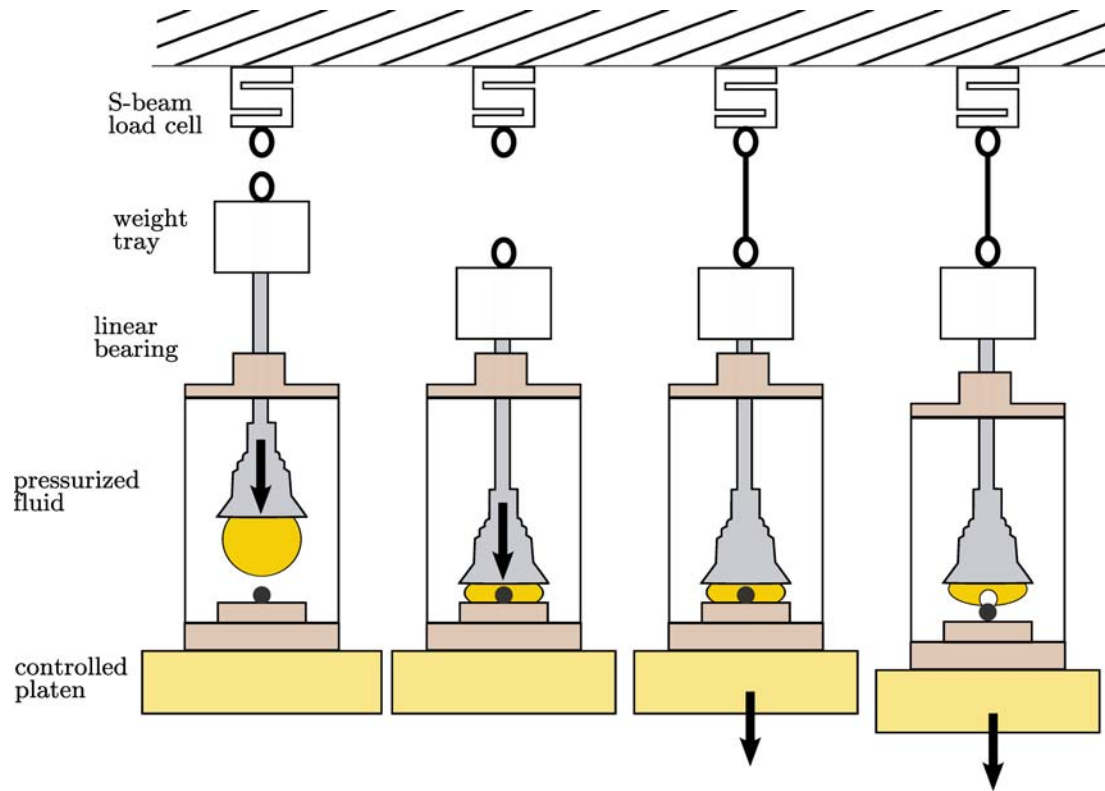


Figure 7: Schematic illustrating motion of gripper and platen during bench top experiments. (a)-(b) The gripper settles on to the object under its own weight until the gripper membrane is jammed. (c)-(d) The gripper shaft is connected to overhead load cell and then the platen is lowered until the gripper completely loses contact with the object. The lifting force is the difference between the maximum vertical load during the downward motion, and the vertical load after the gripper loses contact. Both platen position and load are recorded at 10Hz.

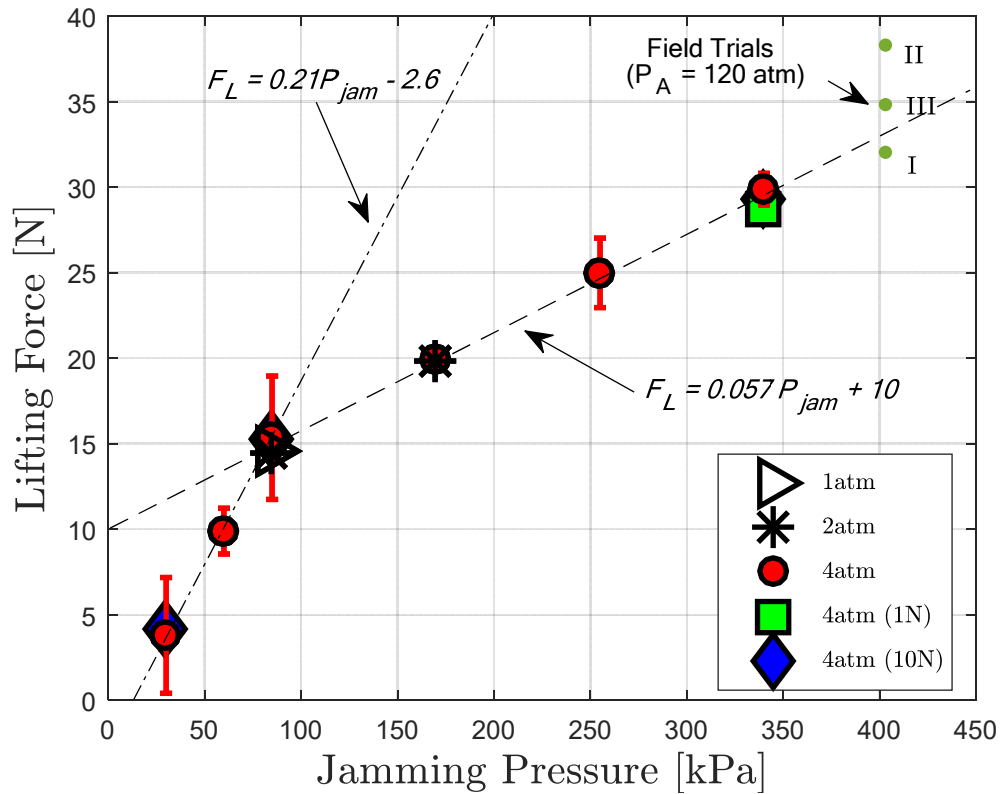


Figure 8: Gripper lifting force,  $F_L$ , is shown at six jamming pressures,  $P_J$  where ambient pressure  $P_A = 4\text{atm}$ , gripper weight  $F_W=5\text{N}$ , and initial fluid volume  $V_I=120\text{mL}$ .  $n=5$  trials per operating point.  $F_L$  is clearly dependent on  $P_J$ , and exhibits a linear relationship for  $P_J > 85\text{kPa}$ , with the linear regressions shown as the dashed lines. Three experiments were performed at reduced ambient pressures:  $P_J=85\text{ kPa}$  at  $P_A=1\text{atm}$ , and  $P_J=(85, 170)\text{ kPa}$  at  $P_A=2\text{atm}$ ; no dependence on  $P_A$  was found. Four experiments were performed with varying in water weight  $F_W=(1, 10)\text{N}$  and three different values of  $P_J$ , no dependence on  $F_W$  was found. Results from three individual field trials of the gripper with  $P_J=4\text{ atm}$  operated at a water depth of 1200m ( $P_A\approx 120\text{ atm}$ ) suggests that the gripper performance remains independent of ambient pressure even at these depths.

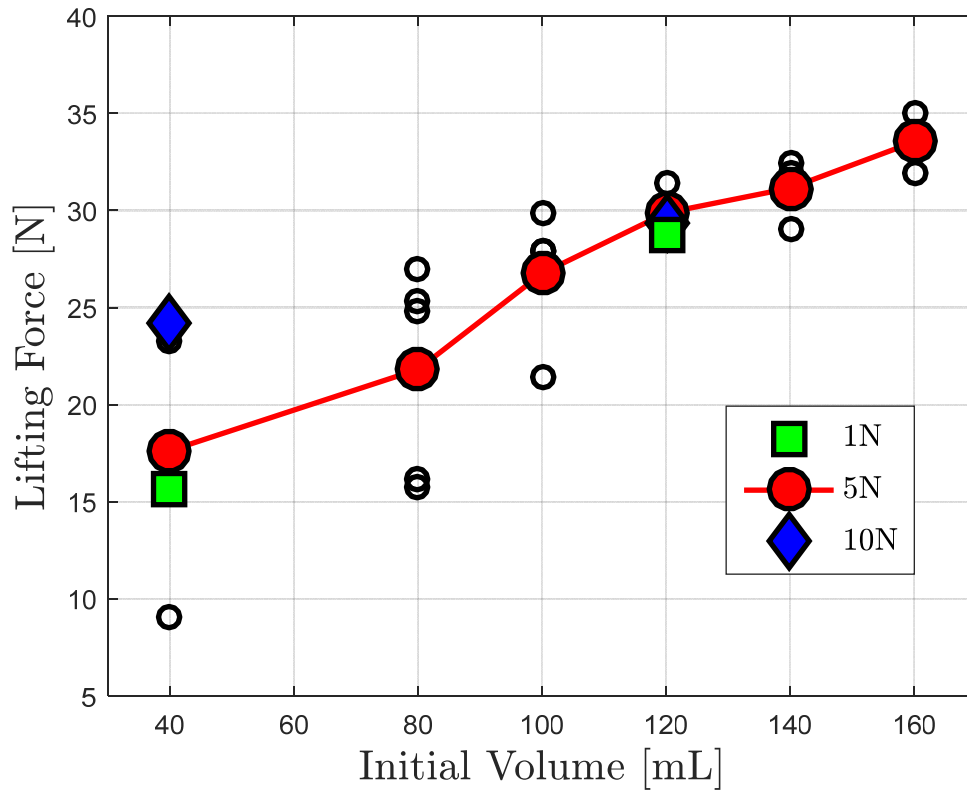


Figure 9: Mean pull strengths,  $F_L$ , for six initial fluid volumes,  $V_i$ , are shown for the case where ambient pressure is 4atm, gripper weight is 5N, and jamming pressure is 340kPa ( $n=5$  trials each). The *mean* pull strength shows a strong dependence on  $V_i$ . Results from all individual trials with gripper weight of 5N are also shown (empty black circles). There appears to be a bimodal distribution of recorded pull strength for  $V_i \leq 100$ mL. Mean results from four experiments with varying gripper weight are also shown, with  $F_W=(1,10)$ N with  $V_i=(40,120)$ mL



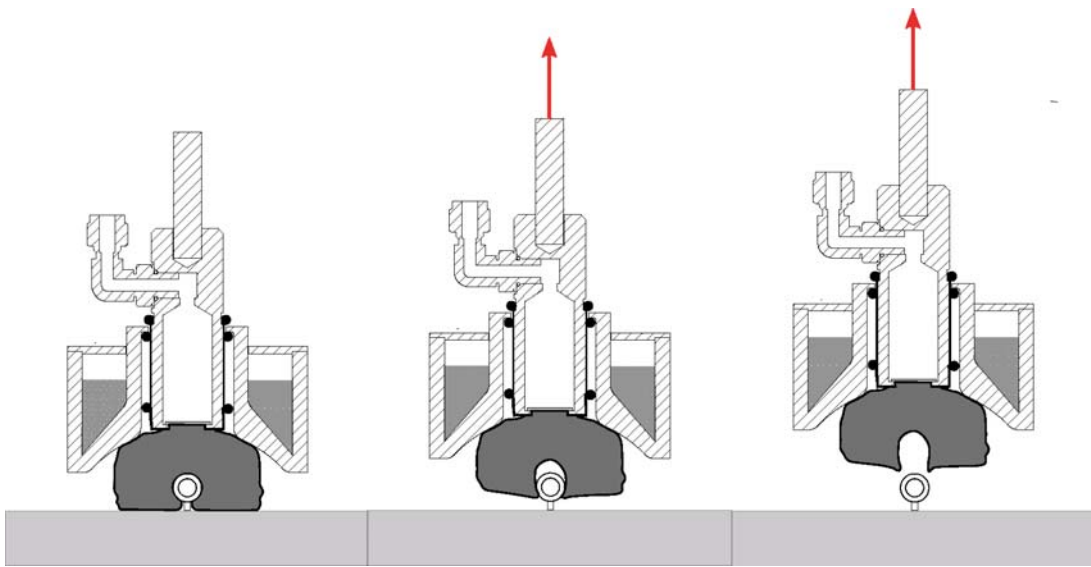


Figure 10: Cross-section showing typical deformation of jammed gripper from initial grasp to release of the sample rod, based in time-lapse video images from the case with jamming pressure  $P_J=340\text{kPa}$ , ambient pressure  $P_A=4\text{atm}$ , initial fluid volume  $V_I=120\text{mL}$ , and in water gripper weight  $F_W=5\text{N}$ . The grip fails through deformation of tabs that extend underneath the sample rod from both sides. The resulting shape can be seen from a bottom view in Figure 14.

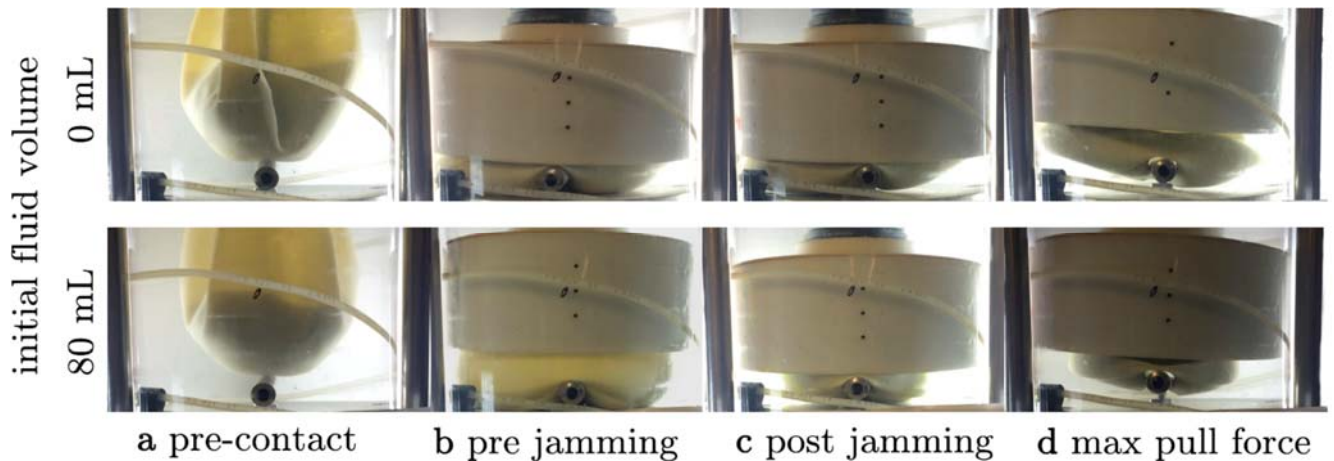


Figure 11: Comparison of membrane shape during grasp with  $V_I=40\text{mL}$  and  $V_I=120\text{mL}$ . (a) Just before contact, the lower initial volume creates deeper folds resulting in a less organized membrane. (b) Prior to jamming, the weight of the gripper is supported by the membrane when  $V_I=120\text{mL}$ , rather than resting directly on the sample through the rigid cap as when  $V_I=40\text{mL}$ . (c) After jamming, the effect of asymmetry for the lower initial volume is evident, with a larger mass of beads situated to one side of the sample than the other. (d) For the higher initial volume, the jammed gripper consistently pulled upward on the sample without rotating or stretching the membrane, as compared to the lower initial volume case where in some cases the jammed gripper experienced significant rotation and stretching.





**a** pre-contact



**b** pre jamming



**c** post jamming



**d** max pull force



**e** release

Figure 12: Estimates of maximum lift forces were derived from video frame captures showing compression of the lower spring, both at maximum compression and shortly after release. Note that while the shaft is obscured by the lower polyurethane ball, the cylinder bearing is not in contact with the fluid manifold in images (a), (c), or (e). Arm motion was manually controlled, resulting in motions that were not perfectly vertical. All operations were performed by the same ROV pilot in an attempt to maintain consistency in speed and accuracy.

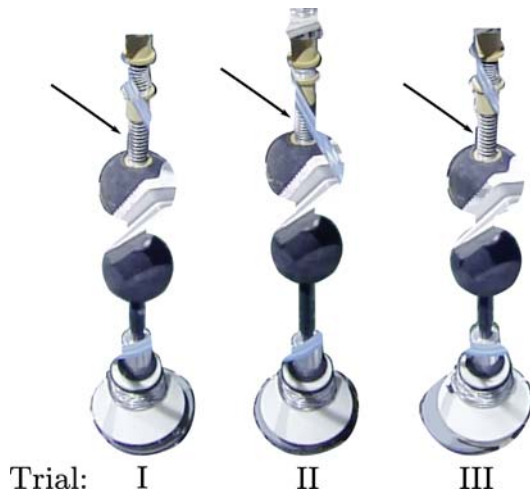


Figure 13: Isolated and rotated images of the gripper from the video frames used to determine vertical force from spring deformation for the three trials performed. Arrow indicates the lower spring in each case. The lower spring has a spring constant  $k=0.60$  N/mm. Variations in camera angle were accounted for using the known along axis length of the spring spacer (1.0in). The estimated vertical forces are 32N, 38N, and 35N for trials I, II, and III, respectively.

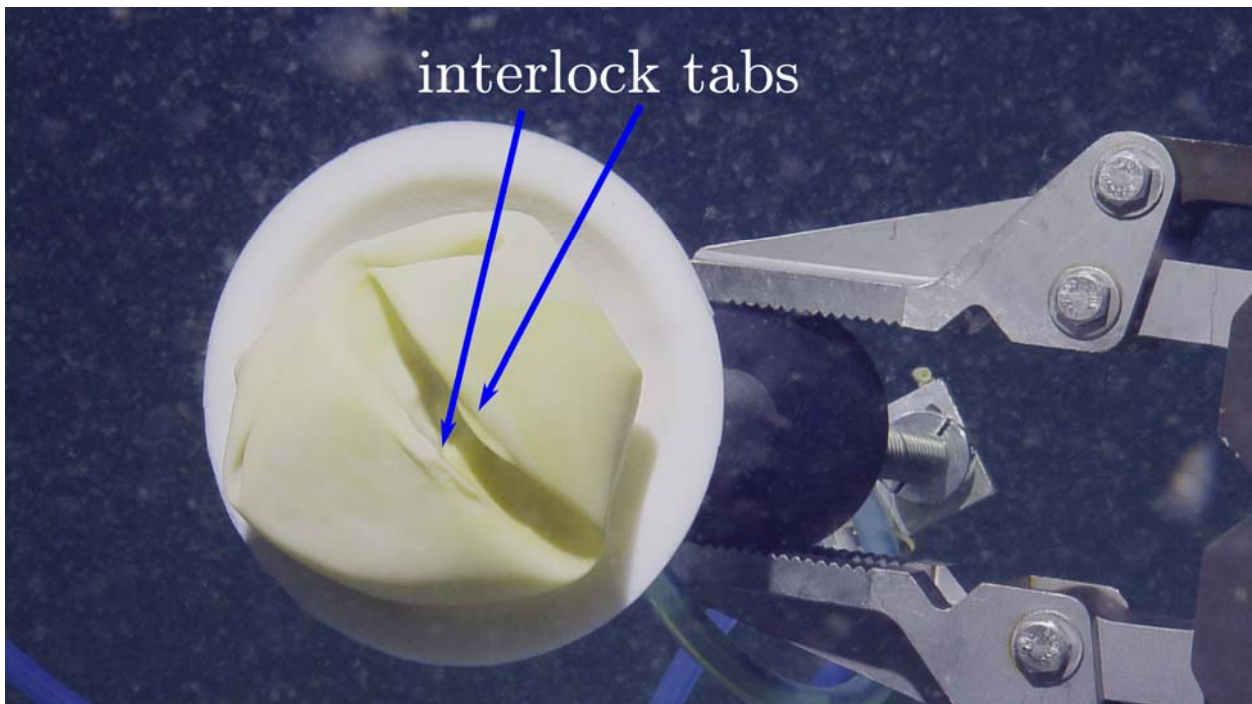


Figure 14: Jammed gripper shape immediately after pulling free from the sample rod during tests at depth on the ROV *Hercules*. The impression of the rod is visible, as well as the deformed 'tabs' that were initially extended under the rod during the approach and grasp. The formation of the tabs indicates that interlock was achieved. To lift the gripper off of the sample, enough force must be applied to sufficiently deform these tabs to allow the object to be released.

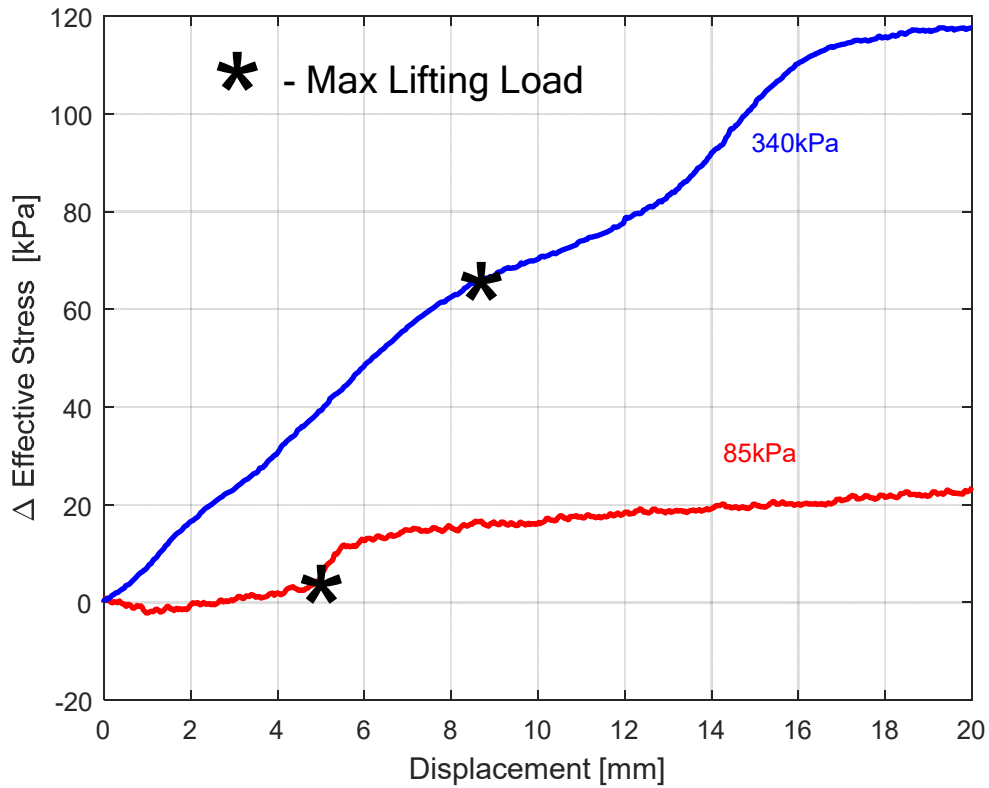


Figure 15: Effective stress change,  $\Delta \sigma'$ , as a function of gripper displacement, at initial jamming pressures,  $P_j=85\text{kPa}$  and  $P_j=340\text{kPa}$ . The pressure occurring at maximum recorded lifting force is highlighted for each. At  $P_j=85\text{kPa}$ , pressure has increased by 5kPa when failure occurs, reducing  $\sigma'$  to 80kPa, a 6% drop from the initial value. At  $P_j=340\text{kPa}$ , the pressure has increased by 65kPa when failure occurs, reducing  $\sigma'$  to 275kPa, a 19% drop from the initial value.